Cortical thickness of left Heschl's gyrus correlates with hearing acuity in adults - A surface-based morphometry study

Neuschwander, Pia ; Hänggi, Jürgen ; Zekveld, Adriana A ; Meyer, Martin

DOI: https://doi.org/10.1016/j.heares.2019.107823

Cortical Thickness of left Heschl's Gyrus Correlates with Hearing Acuity in Adults – A Surface-Based Morphometry Study.

Pia NEUSCHWANDER[a*], Jürgen HÄNGGI[a], Adriana A. ZEKVELD[b] & Martin MEYER[a,c]

[a] University of Zurich, Neuropsychology Division, Department of Psychology, Zurich, Switzerland

[b] Amsterdam UMC, Vrije Universiteit Amsterdam, Otolaryngology – Head and Neck Surgery, Ear & Hearing, Amsterdam Public Health Research Institute, De Boelelaan 1117, Amsterdam, The Netherlands

[c] Tinnituszentrum, Charité - Universitätsmedizin Berlin, Germany

[*] Corresponding author: Pia Neuschwander, University of Zurich, Neuropsychology Division, Department of Psychology, Binzmühlestrasse 14/25, 8050 Zurich, Switzerland, Email: pia.neuschwander@psychologie.uzh.ch

Abstract

To date, research examining the relationship between brain structure and hearing acuity is sparse, especially given the context of a broad age range. To investigate this relationship, we applied an automated surface-based morphometry (SBM) approach (FreeSurfer) in this study to re-examine a sample of normal-hearing (n = 17) and hearing-impaired (n = 17) age- and education-matched adults, aged between 20 and 63 years (Alfandari et al., 2018). The SBM approach allows the disentanglement of cortical surface area (CSA) from cortical thickness (CT), the 2 independent constituents of cortical volume (CV). We extend the findings of Alfandari and colleagues by showing several clusters in auditory-related areas as well as in the left and right angular gyrus that showed reduced CT, CSA and CV in hearing-impaired compared to normal-hearing listeners. Nevertheless, none of the clusters found correlated significantly with hearing acuity, measured by pure-tone thresholds, in the 2 groups. An additional vertex-wise correlation analysis between hearing acuity and morphometric parameters over all participants revealed a single significant cluster encompassing the left Heschl's gyrus. Higher hearing thresholds were associated with a thinner cortex within this cluster. Our results imply that hearing impairment is associated with reduced thickness in primary and secondary auditory cortex regions, those regions especially involved in perceiving and processing relevant speech cues. This

decrease was observed not only in older but also in younger and middle-aged adults, independent of age-related decline in the cognitive domain and age-dependent whole-brain atrophy. Further, the results show the value added when considering CV, CT and CSA separately, relative to previous studies which have solely relied on voxel-based morphometry to investigate brain structure and hearing acuity across the lifespan.

Keywords: hearing loss, structural plasticity, cortical thickness, Heschl's gyrus, surface-based morphometry

1. Introduction

Contrary to the widely held belief that hearing loss is part of the normal aging process and thus affects only older adults, the prevalence of hearing loss indicates exactly the opposite of what most would expect based on this assumption. As the Institute for Better Hearing stated in 2014, the majority of people with hearing loss (65%) are younger than 65 (Associated Hearing Care, 2019). In addition, in recent years, the number of adults with peripheral hearing loss occurring at an early age has increased. For example, a study by Shargorodsky, Curhan, Curhan, and Eavey (2010) on the incidence of peripheral hearing loss in US adolescents aged 12 - 25 years showed an increase from 14% in 1994 to 19% in 2006. The scholars assume that one reason for this trend could be an increased noise exposure in daily life and the excessive use of personal audio devices, such as headphones at ear level (Shargorodsky et al., 2010). This increasing trend is not limited to the US. Various studies of the World Health Organization (WHO) have shown that even though peripheral hearing loss often occurs in combination with old age (i.e., so-called presbycusis), there is also a world-wide trend that younger adults under the age of 60 years more frequently report difficulties in understanding speech than in previous years. The WHO relates this increase to excessive noise exposure or noise trauma (WHO, 2018).

Even though peripheral hearing loss affects not only older adults, most studies still focus on middle-aged to elderly people when investigating the relationship between neuroplasticity and hearing acuity (e.g., Cardin, 2016; Mudar & Husain, 2016). Several studies that examined this relationship in older adults showed a relationship between increasing severity of peripheral hearing loss and reduced gray matter (GM) volume in auditory cortex areas (Eckert et al., 2012; Husain et al., 2011; Peelle et al., 2011). In particular, these studies suggested that the volume of gray matter (GM) in the left auditory cortex is associated with age-related high-frequency hearing loss (Eckert, et al., 2012). Furthermore, longitudinal studies showed accelerated rates of decline in GM volume in the right temporal lobe for older-aged adults suffering from peripheral hearing loss (Lin et al., 2014), and a relationship between hearing impairment and decreased total brain volume and smaller white matter (WM) volume in the elderly (Rigters et al., 2017).

In contrast, studies with middle-aged adults who suffer from peripheral hearing loss revealed that poorer

hearing thresholds were associated with increased GM volume in the temporal and limbic lobes and decreased GM volume in the frontal lobe (Boyen et al., 2013). Further studies showed associations between decreased WM volume and increased severity of peripheral hearing loss (Chang et al., 2004; Husain et al., 2011).

A closer look at the literature confirms that both peripheral hearing loss and its consequences on brain anatomy in middle to old age has already been well-documented. Changes in brain anatomy caused by early-onset deafness in infancy have also been intensively studied (Glick & Sharma, 2017). In deaf people, brain structures that normally process auditory input, such as the primary auditory cortex (Heschl's gyrus), secondary auditory cortex (Heschl's sulcus) and third auditory cortex (planum temporale, superior temporal gyrus), are subject to reorganization. These areas become associated with the processing of information received by the intact senses and respond to visual, tactile and sign language input (Glick & Sharma, 2017; Petitto et al., 2000). Further, studies investigating neuroanatomical alterations in children with peripheral hearing loss showed WM lesions associated with hearing loss (Joshi et al., 2012) as well as significant reduced cortical thickness in hearing-impaired compared to normal-hearing children and teenagers (Li et al., 2012). According to the above-mentioned literature, the relationship between age-related peripheral hearing loss and brain plasticity in middle- to older-aged people has also already been well studied (e.g., Mudar & Husain, 2016). Additionally, there are also findings in the area of brain plasticity caused by premature deafness or early peripheral hearing loss (e.g., Joshi et al., 2012). However, there appears to be a lack of studies that comprehensively investigate the relationship between anatomical parameters and peripheral hearing loss over a broader age range (i.e., from younger to older people). Therefore, at present the knowledge regarding the brain changes that underline the adaptive strategies applied by people with peripheral hearing loss to understand speech is still sparse, and neither the direction of the hearing-loss-related changes (i.e., an increase or decrease of neuroanatomical parameters) is clear, nor is it yet clarified which brain regions are directly involved. This observation holds particularly true given a broader age range. Thus, the aim of this study was to shed more light on the relationship between brain plasticity and hearing acuity by re-analyzing a dataset provided by Alfandari et al. (2018) with a complementary morphometric method. In their study, Alfandari and co-authors used an exploratory voxel-based morphometry (VBM) analysis

to investigate whether hearing impairment was associated with differences in brain volume. With our study, we seek to extend the findings of Alfandari et al. (2018) by means of a surface-based morphometry (SBM) approach, which allows us to explore additional morphometric parameters besides cortical volume (CV), namely the CV constituents that are cortical thickness (CT) and cortical surface area (CSA) (Meyer et al., 2014; Panizzon et al., 2009; Winkler et la., 2010). We compared the data from a group of normal-hearing (NH) listeners with an age- and education-matched group of hearing-impaired (HI) listeners between 20 and 63 years of age. Based on the results of Alfandari et al. and other studies (e.g., Meyer et al., 2014; Profant et al., 2014; Giroud et al., 2018), we conducted a region of interest analysis (ROI) within seven regions encompassing the perisylvian cortex that are known to mediate spoken language. We checked that all participants in the chosen age range do not show any remarkable signs of age-related cognitive decline or age-related atrophy. Therefore, the data set allowed us to assess how peripheral hearing loss may be associated with cortical brain structures in core auditory regions, independent of age-related decline in the cognitive domain as well as in terms of brain atrophy.

1.1 Surface-Based Morphometry Method

At present, there are several studies that investigated the relationship between brain structure and hearing impairment, focused on the older population (e.g., Cardin, 2016; Eckert et al., 2012; Husain et al., 2011; Mudar & Husain, 2016; Peelle et al., 2011). The majority of these used VBM to analyze differences in GM and WM volume in the whole brain or in different regions of interest (see literature overview described above). In the current study, we chose an alternative approach to investigate morphometric differences between hearing-impaired and normal-hearing listeners. We applied an established SBM approach, namely the FreeSurfer analysis software suite (Dale et al., 1999; Dale et al., 2002; Fischl, 2012). This software allows for the separate examination of CT and CSA, thus resulting in a more differentiated and detailed picture of the relationship between peripheral hearing loss and cortical anatomy than is possible in the more common VBM approach.

According to Panizzon et al. (2009), as CV is estimated by computing the product of CSA and CT, it is arguable that, if CSA and CT may run in opposite directions, the resulting CV measurement could be confounded and hearing-loss-related alterations, for example, might be overseen (Meyer et al., 2016; Panizzon et al., 2009). Thus, SBM is an appropriate approach as its specificity allows for both CT and

CSA to be quantified, meaning that subtle differences in the relationship between CT and CSA can be detected. The extracted CT in SBM is a correlate for the distance between the gray/white matter border and pial surfaces and thus represents a direct measure of the amount of gray matter present at each point on the surface (Greve, 2011). CSA on the other hand is defined as the mean area of the triangular region at the respective surface data point (or vertex) (Meyer et al., 2016). Like the measure for GM concentration in VBM, CT and CSA can be used in a group analysis to track changes that are associated with age or disease processes (Greve, 2011). According to the Radial Unit Hypothesis (Rakic, 1988, 1995, 2007), cortical thickness and cortical surface area should be considered as independent traits that have different genetic origins. Further, compared with CSA or CV, CT is more sensitive to the dynamic modulations associated with training and experience over the lifespan (Bermudez et al., 2009; Engvig et al., 2010; Schneider et al., 2009; Strosve et al., 2014), a characteristic which makes it especially interesting to investigate in combination with hearing loss. As outlined above, no studies as yet have investigated the relationship between CT and hearing impairment over a broader age range. However, changes in CT in association with hearing loss have been shown in young children and adolescents who suffer from severe hearing loss (Li et al., 2012). In an SBM study, Li et al. (2012) showed significant reduced CT in HI compared to NH children and teenagers aged between 10 and 18 years. CT of the impaired children suggested significantly thinner areas in the left precentral gyrus, right postcentral gyrus, the left superior occipital gyrus and the left fusiform gyrus compared with the normal-hearing children (Li et al., 2012). In addition, Giroud et al. (2018) observed that reduced CT may be associated with “hidden hearing loss” in older adults as well. Hidden hearing loss is a term used to describe problems understanding speech in noise given the absence of peripheral hearing loss. Giroud et al. showed that older adults suffering from hidden hearing loss showed reduced CT in auditory-related areas as well as in frontal areas when compared to a normal-hearing younger control group. Additionally, the authors found a positive correlation between CT in auditory-related areas and performance in suprathreshold auditory tasks in older adults (Giroud et al., 2018). Further, Liem et al. (2014) showed a relationship between CT and auditory performance in younger adults. Specifically, participants with a thicker left auditory-related cortex (planum polare) performed better on an in-scanner auditory pattern matching task compared to participants with a thinner planum polare (Liem et al.,

2014). To our knowledge, there are so far no further studies that have used SBM to investigate anatomical differences and hearing loss. Therefore, our study is one of the first to describe possible neuroanatomical differences between NH and HI adults over a broader age range using an SBM approach.

When taken together and considered independently of the analysis approach applied (VBM or SBM), the currently available evidence suggests altered structural parameters in auditory-related areas in HI listeners compared to NH listeners as a function of hearing loss. However, the degree to which the reported changes are due solely to peripheral hearing impairment is difficult to determine, and one aspect of this difficulty is the lack of appropriate age-matched control groups spread across a wider age range. In a former VBM analysis of the exact same dataset as was analyzed in the current study, Alfandari et al. (2018) compared GM and WM volumes between the NH control group and the HI participants. They used exploratory whole-brain as well as post-hoc region of interest analyses to investigate differences in brain structures associated with spoken language processing. The results showed increased GM volume in the right angular gyrus and decreased WM volume in the left fusiform gyrus in HI listeners when compared to the NH group (Alfandari et al., 2018). Additionally, these authors found a significant correlation between increased severity of hearing loss and increased GM volume of the right angular gyrus in the HI group. According to Alfandari et al., these results can be interpreted as indicating a link between partial hearing loss and altered brain volume. To find evidence that is not as restricted in terms of brain volume parameters for this observed link, we will re-analyze the same dataset with an ROI-based SBM approach that makes the analysis of additional informative parameters possible. As mentioned above, Alfandari et al. (2018) did not find any associations between auditory-related areas and hearing acuity, a finding which could be due to the applied VBM approach. Therefore, for our SBM analysis we hypothesized that peripheral hearing loss is accompanied by CT/CSA alterations in auditory-related brain areas (perisylvian region), such as Heschl's gyrus (HG), Heschl's sulcus (HS), superior temporal gyrus/sulcus (STG/STS), planum polare (PP) and planum temporale (PT), as these are the most likely regions to be associated with hearing loss induced changes. Because it seems that CT especially is sensitive to change (Bermudez et al. 2009; Engvig et al. 2010), our main assumption was that we would find a relationship between CT and the severity of hearing loss.

2. Method

2.1 Participants

We re-analyzed the dataset collected by Alfandari et al. (2018). In total, 17 adults with age-typical normal-hearing (5 males, 12 females; *M* = 45.88 years, *SD* = 15.56 years, age range: 20 – 62 years) and 17 adults with peripheral hearing impairment (HI: 5 males, 12 females; *M* = 45.65 years, age range: 20 – 63 years, *SD* = 15.66 years) participated in the study. HI and NH participants were individually matched based on age and educational level. Fourteen of the 17 participant pairs were individually matched based on sex, and the ratio of males to females was matched between the groups (see Alfandari et al., 2018). Participants with NH were recruited from the staff and students of the Vrije Universiteit (VU) medical center and the VU Amsterdam, the Netherlands. All participants showed pure-tone thresholds of maximal 20 dB at the octave frequencies between 500 and 4000 Hz. The mean pure-tone average (mPTA; mean hearing threshold at 500, 1000, 2000, and 4000 Hz, averaged over both ears) of the participants with normal-hearing was 5.5 dB HL (*SD* = 5.5, range: 5 to 18.3 dB HL). Average thresholds at 8000 Hz were 17.94 dB HL (*SD* = 16.45, range: 2.5 to 45 dB HL; see Figure 1 for the average air conduction hearing thresholds at the octave frequencies between 250 and 8000 Hz). Participants with hearing impairment were recruited among the patients of the outpatient clinic of the Ear Hearing section of the Department of Otolaryngology - Head and Neck Surgery of the VUmc. All participants with hearing impairment had symmetrical peripheral hearing loss (Alfandari et al., 2018). For inclusion in the study, the mPTA of each ear in the HI group was required to be between 35 and 65 dB HL. Also, the asymmetry in the pure-tone thresholds between both ears could not exceed 20 dB at one, 15 dB at two, or 10 dB at three of the octave frequencies between 250 and 4000 Hz. The mPTA of the group with hearing impairment was 49.8 dB HL (*SD* = 7.3, range: 40 – 61.6 dB HL). Thresholds at 8000 Hz were on average 50.88 dB HL (*SD* = 22.32, range: 12.5 – 97.5 dB HL). The etiologies of the impairments included combinations of congenital (*n* = 2), familial (*n* = 6), noise-induced (*n* = 2), and age-related (*n* = 6) hearing loss. One participant reported perinatal asphyxia as the suspected etiology, and four participants reported unknown causes (Alfandari et al., 2018). Diagnosed hearing impairment showed an average duration of 17 years (range: 1 – 43 years, *SD* = 12 years). Duration and severity of hearing impairment did not correlate significantly ($r = 0.42$, $p = 0.09$). Neither duration nor severity

correlated significantly with age ($r = 0.46$, $p = 0.06$ and $r = 0.19$, $p = 0.46$, respectively). All air-bone gaps were smaller than 10 dB (see Figure 2) and all participants had normal tympanograms (Alfandari et al., 2018). On a speech audiogram with standard monosyllabic Dutch consonant–vowel–consonant word lists, all participants scored better than 80% on each ear (Bosman and Smoorenburg, 1995). Furthermore, all participants were native Dutch speakers who used only spoken language and no sign language. All were classified as right-handed by the Dutch "Classification of left and right-handed subjects" (van Strien, 1992). They had normal or corrected-to-normal vision and were screened by a near-vision test that is equivalent to the visual acuity Snellen chart (Bailey and Lovie, 1980). Exclusion criteria of the study were the use of psychotropic medication, a history of a neurological/psychiatric disease, reading problems (e.g., dyslexia), claustrophobia, epilepsy, pregnancy, or metal in the body contraindicating MRI scanning. All participants provided written informed consent, and the study was approved by the Ethics Committee of VU medical center (Alfandari et al., 2018).

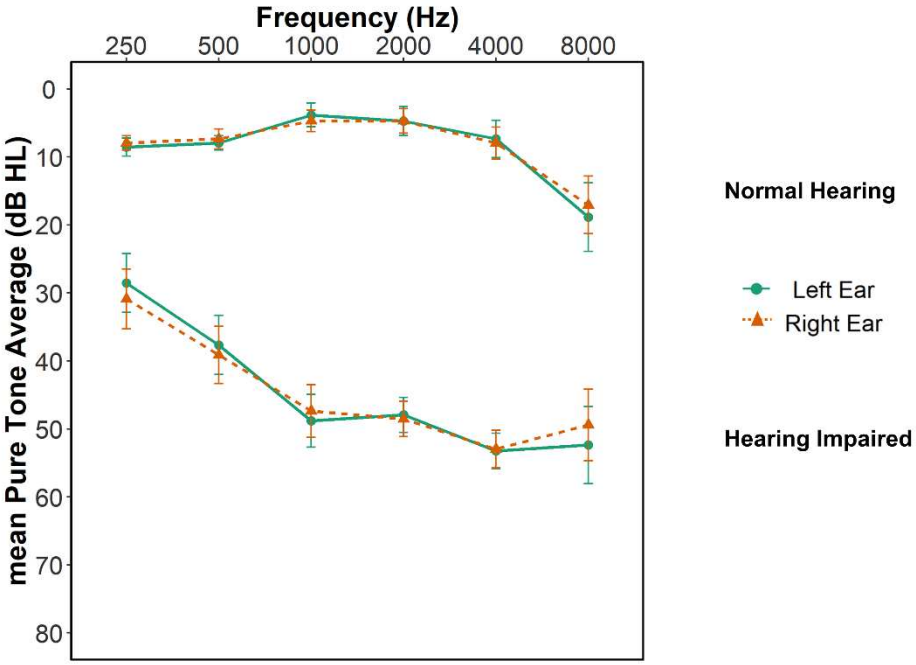

Fig. 1. Average pure-tone (air conduction) hearing thresholds at the octave frequencies between 250 and 8000 Hz for both participant groups and both ears separately. Error bars show the standard error of the mean.

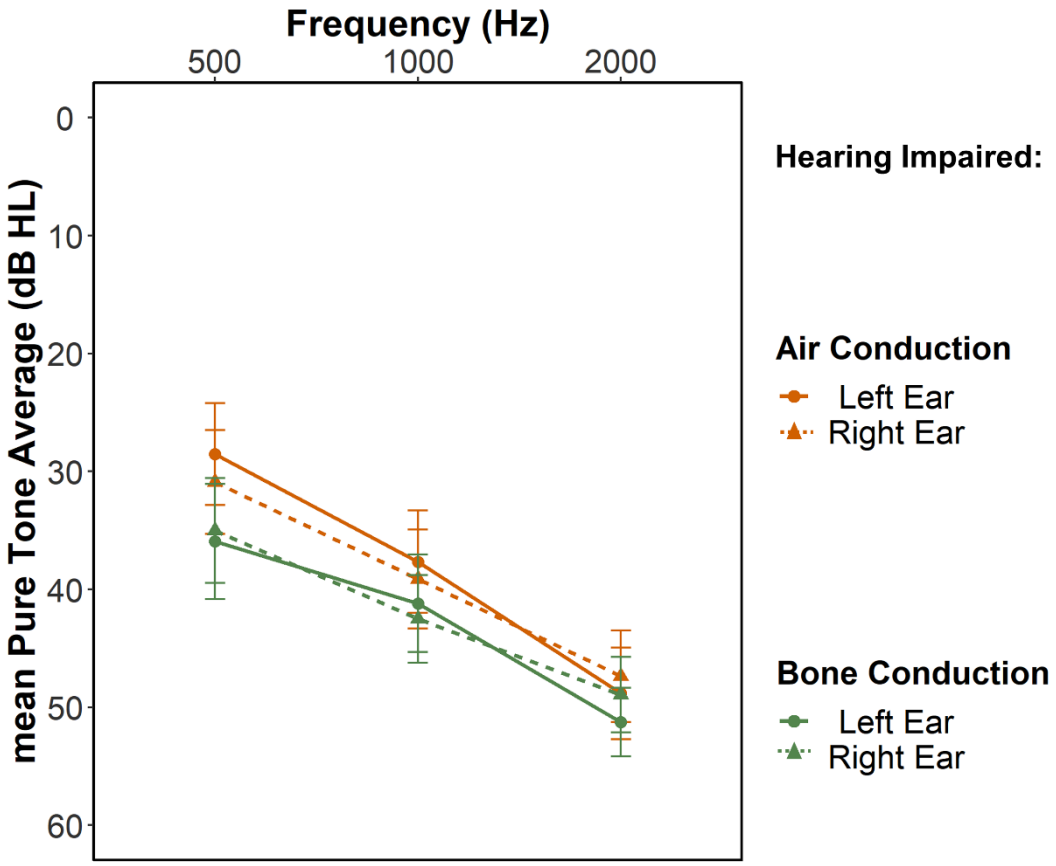

Fig. 2. Average air and bone conduction hearing thresholds at the octave frequencies for 500, 1000 and 2000 Hz for the hearing-impaired group for both ears separately. Error bars show the standard error of the mean.

2.2 MRI Data Acquisition

The T1-weighted MRI scans were obtained using a 3T GE Signa scanner (General Electric Company, Fairfield, CT, USA), equipped with an eight-channel phased head coil array, using a fast spoiled gradient-recalled echo sequence with the following parameters: repetition time = 8.236 ms, echo time = 3.248 ms, inversion time = 450 ms, flip angle = 12°, field of view = 220 mm^2, 166 sagittal slices, spatial resolution = 1 mm x 0.9 mm x 0.9 mm. Total scan time was approximately 5 minutes.

2.3 Surface-Based Morphometry Analysis

Cortical surface reconstruction and volumetric segmentation were performed with the FreeSurfer image analysis suite (version 6.0; Fischl, 2012). The software is documented online and freely available for download (https://surfer.nmr.mgh.harvard.edu/). The surface-based morphometry analysis implemented

in the FreeSurfer pipeline comprises several pre-processing steps. The technical specifications of these pre-processing steps have already been described in detail in previous publications (e.g., Dale et al., 1999; Dale & Sereno, 1993; Fischl et al., 2001; Fischl & Dale, 2000; Fischl, Sereno, & Dale, 2002; Segonne et al., 2004; Sled et al., 1998;). After motion correction, the automatic pre-processing in FreeSurfer performs a non-parametric non-uniform intensity normalization (N3) (Sled, Zijdenbos, & Evans, 1998). This well-known intensity inhomogeneity correction method is iterative and seeks the smooth multiplicative field that maximizes the high frequency content of the distribution of tissue intensity (Sled, Zijdenbos, & Evans, 1998). The method is fully automatic, requires no a priori knowledge and can be applied to almost any MR image. According to Vovk, Pernus & Likar (2007), this method is one of the most successful and popular methods for intensity inhomogeneity correction. The automatic parcellation of the cerebral cortex into units based on gyral and sulcal structure was performed using Destrieux's aparc.a2009s annotation (Destrieux et al., 2010). Finally, morphometric parameters such as the total CV, mean CSA and the mean CT were extracted. To assess the quality of the conducted pre-processing steps, the quality assessment tools implemented in FreeSurfer were used. SNR ratios were comparable between groups ($t(32) = -1.05$, $p = 0.30$). For the statistical group analysis, the reconstructed images were morphed to an average spherical surface template (fsaverage) and were then spatially smoothed with a 10 mm full-width-half-maximum Gaussian kernel. The resulting surface models were not manually edited.

2.4 Statistical Analyses

2.4.1 FreeSurfer Vertex-Wise Group Comparison

To test whether the two groups showed any anatomical differences, we first conducted a FreeSurfer vertex-wise group comparison between the NH and the HI participants. For better comparability with the previous VBM analysis conducted by Alfandari et al. (2018), the same ANCOVA model as in the VBM analysis was used, with one group factor (HI vs. NH) and age as covariate. However, in contrast to the VBM analysis, we did not use a global control variable like mean/total thickness/area/volume as an additional covariate, because none of these control variables differed significantly between the two groups (see Table 1). After fitting the GLM with the built-in function in FreeSurfer, we ran 5,000 Monte-Carlo simulations to correct for multiple comparisons at the cluster level (Hayasaka & Nichols,

2003) as implemented in FreeSurfer (Hagler et al., 2006). For the simulations, the cluster-wise (corrected) threshold was set to $p = 0.05$. Statistical analysis was conducted vertex-wise within the defined ROIs (see Figure 3). To define the chosen regions, the aparc.a2009s annotation was used (Destrieux et al., 2010). This labelling procedure allows to annotate separate regions for the Heschl's gyrus (HG), Heschl's sulcus (HS), superior temporal gyrus/sulcus (STG/STS), planum polare (PP), planum temporale (PT) and the angular gyrus (AG). However, because the HG exhibits a highly variable morphology (Brodmann 1909; Celesia 1976; Von Economo and Horn 1930; Galaburda and Sanides 1980; Marie et al., 2015; Schneider et al., 2002) that includes one to three gyri per hemisphere, with the number of gyri varying between hemispheres (Campain and Minckler 1976; Von Economo and Horn 1930;Pfeifer 1920), it is important to note that in case of such potential HG duplications or triplications, these additional transverse temporal gyri, made of secondary auditory cortex (Shapleske et al., 1999), were included in the parcellation of the planum temporale (Destrieux et al., 2010). For the sake of completeness, the region-wise mean values of all seven regions of interest can be found in the appendix A (see Table A1, A2 and A3).

Table 1: The mean (*M*) and standard deviation (*SD*) of global variables for cortical volume, cortical thickness and cortical surface area, separately for hearing-impaired and normal-hearing participants. The *t* tests indicate differences between participant groups.

	Hearing Impaired		**Normal Hearing**		*t*	$P_{FDRadj.}$
	M	*SD*	*M*	*SD*		
Estimated total intracranial volume	1424960.56	114670.21	1439961.57	117334.77	$t(32) = 0.004$	0.801
Mean cortical thickness RH	2.54	0.08	2.57	0.12	$t(32) = 3.312$	0.778
Mean cortical thickness LH	2.55	0.07	2.58	0.11	$t(32) = 5.569$	0.778
Mean cortical surface area RH	81202.86	5534.13	81889.38	7614.49	$t(32) = 1.183$	0.801
Mean cortical surface area LH	81469.53	5403.09	82017.22	7070.5	$t(32) = 0.498$	0.801

Note. RH = right hemisphere, LH = left hemisphere, , $p_{FDRadj.}$ = FDR adjusted *p* value.

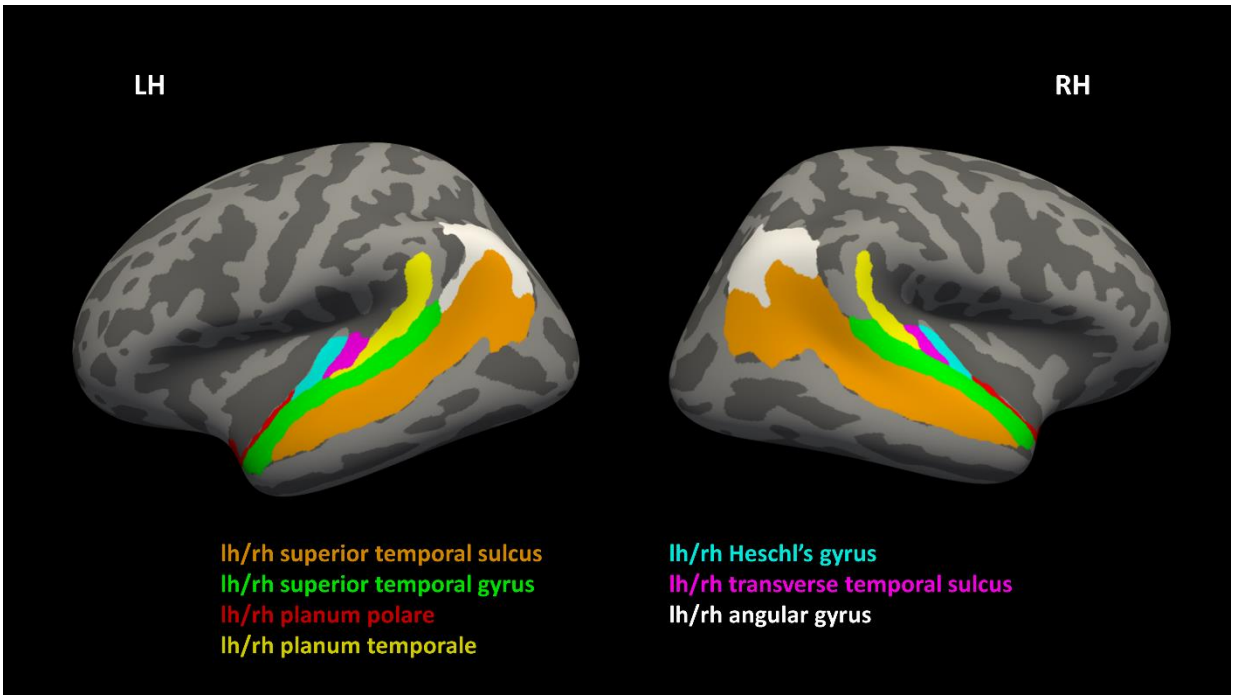

Fig. 3. Defined regions for the ROI analysis, selected according to Alfandari et al. (2018), Meyer et al. (2013), and Profant et al. (2014). The parcellation of the cerebral cortex was performed using Destrieux's aparc.a2009s annotation (Destrieux et al., 2010). LH = left hemisphere, RH = right hemisphere.

2.4.2 Cluster-Wise Correlation Analysis

In a next step, we conducted a cluster-wise correlation analysis to check whether possible anatomical differences between the NH and HI groups revealed by the vertex-wise group comparison were associated with the severity of hearing loss. We therefore chose all clusters that significantly differed between the groups as a result of the previously conducted analysis (see 2.4.1) and extracted for each of these the estimated vertex-wise CV, CT and CSA. For each group, we correlated these values with the severity of hearing loss (mean PTA, measured in dB) separately. Age was used as a covariate of no interest.

2.4.3 FreeSurfer Vertex-Wise Correlation Analysis with Hearing Acuity

Due to the fact that we expected the analytical power to be insufficient because of the relatively small sample sizes of the two groups, we decided to perform an additional vertex-wise partial correlation analysis between morphometric parameters and hearing acuity across the two participant groups in an effort to attain higher statistical power. This additional analysis allowed us to investigate the relationship between brain anatomy and hearing acuity across all participants independent from a

clinical classification for hearing loss/no hearing loss. For this additional analysis we used mPTA as a continuous variable to fit the GLM for all participants and used age as a covariate of no interest in the model. After fitting the GLM with the built-in function in FreeSurfer, we again ran 5,000 Monte-Carlo simulations to correct for multiple comparisons at cluster level (Hayasaka and Nichols, 2003). For the simulations, the initially cluster-forming threshold was set to $p = 0.05$.

2.4.4 FreeSurfer Region-Wise Correlation Analysis with Hearing Acuity

In addition to the vertex-wise partial correlation analysis, we also conducted a region-wise analysis to test the relationship between the mean CV, CT and CSA of each region of interest and hearing acuity. Therefore, we extracted the mean values of CV, CT and CSA in all seven regions of interest (see Figure 3) and conducted a partial correlation between these values and the mPTA, with age as control variable across all 34 participants. The motivation behind this analysis on the region level was to support the findings of the previous analysis on the vertex level.

3. Results

3.1 Vertex-Wise Group Comparison

The vertex-wise group comparison revealed six clusters within our ROIs that differed significantly between NH and HI listeners (see Table 2 and Figure 4). All significant clusters showed decreased values in all measured anatomical parameters for the HI group compared with the participants with normal hearing. For the left hemisphere, we found two significant volume clusters in the superior temporal sulcus (*CWP* = 0.0024, *r* = -0.49) and angular gyrus (*CWP* = 0.0418, *r* = -0.31). Further, the analysis revealed a significant cluster for CT in the superior temporal gyrus/planum polare region (*CWP* = 0.0002, *r* = -0.59) and a cluster for CSA in the superior temporal sulcus (*CWP* = 0.03, *r* = -0.34). For the right hemisphere, the analysis showed two significant clusters, one for volume in the angular gyrus (*CWP* = 0.0094, *r* = -0.41) and one for thickness (*CWP* = 0.0318, *r* = -0.33) located in the angular gyrus/superior temporal sulcus region.

Table 2: Clusters that differed significantly in cortical volume, cortical thickness or cortical surface area between hearing-impaired and normal-hearing participants revealed by ROI analyses. Contrast: HI < NH.

Measure		**Annotation**	**Max**	**NVts**	**Size (mm^2)**	**MNI**			***CWP***	***r***
						X	**Y**	**Z**		
LH	volume	superior temporal sulcus	-4.38	881	441.79	-48	-63	6	0.0024	-0.49
		angular gyrus	-2.43	498	289.47	-40	-75	29	0.0418	-0.31
	thickness	superior temporal gyrus/ planum polare	-2.35	804	502.77	-45	14	-28	0.0002	-0.59
	area	superior temporal sulcus	-2.89	643	330.19	-48	-63	7	0.03	-0.34
RH	volume	angular gyrus	-3.28	616	341.51	40	-68	45	0.0094	-0.41
	thickness	angular gyrus/superior temporal sulcus	-2.23	565	277.05	54	-52	32	0.0318	-0.33

Note. LH: left hemisphere, RH: right hemisphere, Max: log10(p) at peak vertex, NVts: number of vertices above threshold, *CWP*: cluster-wise *p* value of Monte Carlo simulation, *r*: effect-size.

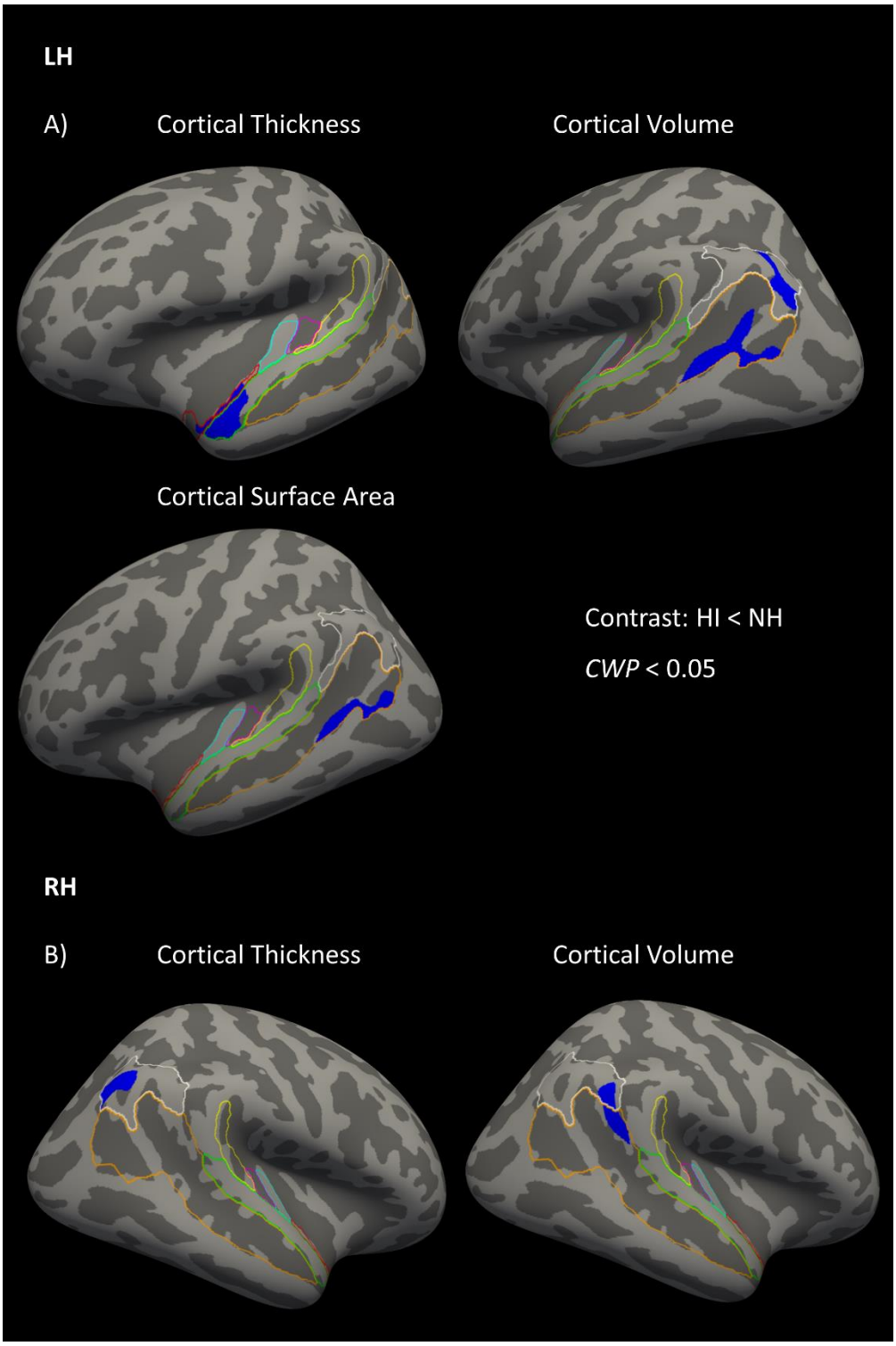

Fig. 4. Clusters that significantly differ between the normal-hearing (NH) and hearingimpaired (HI) group revealed by the ROI analysis. Blue (negative) values indicate reduced morphometric parameters for the HI group. A) Results for the left hemisphere for cortical thickness, cortical surface area and cortical volume. B) Result for the right hemisphere for cortical thickness and cortical volume. ROI annotations according to Destrieuxs aparc.a2009s atlas: light blue = Heschl's gyrus, pink = Heschl's sulcus, red= planum polare, yellow = planum temporale, orange= superior temporal sulcus, green= superior temporal gyrus, white =gyrus angularis. LH = left hemisphere, RH = right hemisphere, CWP = cluster-wise p value.

3.2. Group Comparison: Correlation between Brain Morphometry and Hearing Acuity

To assess whether the anatomical differences between the NH and HI group revealed by the vertex-wise group comparison in section 3.1 were associated with the severity of hearing loss, we conducted a cluster-wise correlation analysis. For both NH and HI, we ran partial correlation analyses between the estimated cluster-wise CV, CT and CSA values on one hand and mPTA on the other hand, with age as control variable. To control for the false discovery rate in multiple testing, we used Benjamini and Hochberg's FDR-controlling procedure (see Benjamini & Hochberg, 1995) and report the adjusted *p* values. Due to the nature of the controlling procedure, it is possible that different uncorrected *p* values show the same adjusted *p* values (see Benjamini & Hochberg, 1995). For both the HI and NH groups, the correlation analyses revealed no significant associations between brain anatomy and severity of hearing loss (see Table 3), not for CV, CSA, or CT.

Table 3: Partial correlation analyses between the clusters that significantly differed between groups (see ROI analyses in Table 1) and mean pure-tone averages for the HI and NH group, controlling for age.

			Hearing Impaired mPTA		**Normal Hearing** mPTA	
			r	$p_{FDRadj.}$	*r*	$p_{FDRadj.}$
RH	thickness	angular gyrus/ superior temporal sulcus	0.25	0.47	-0.48	0.20
	volume	angular gyrus	-0.01	0.97	-0.54	0.18
LH	thickness	superior temoral gyrus/planum polare	-0.44	0.15	-0.44	0.16
	area	superior temporal sulcus	-0.08	0.94	-0.44	0.17
	volume	superior temporal sulcus	0.34	0.30	-0.57	0.24
	volume	angular gyrus	0.06	0.60	-0.46	0.18

Note. RH = right hemisphere, LH = left hemisphere, mPTA = mean pure tone average, $p_{FDRadj.}$ = FDR adjusted *p* value, *r* = correlation coefficient.

3.3 Vertex-Wise Correlation Analysis with Hearing Acuity

The additionally conducted vertex-wise partial correlation analysis between the morphometric parameters and hearing acuity across all 34 participants within the defined ROIs revealed a cluster in the left transverse temporal region (*CWP* = 0.0056, *r* = -0.44), in which poorer hearing acuity was associated with reduced CT (see Table 4). According to Destrieux's aparc.a2009s atlas (2010), this LH cluster included Heschl's gyrus, parts of Heschl's sulcus, parts of the planum polare, parts of the

superior temporal gyrus and a small part of the superior temporal sulcus (see Figure 5). The relationship between CT in this cluster, covering the left transverse temporal region, and mPTA is depicted with a scatterplot in Figure 6.

Table 4: Cluster that correlates significantly negatively in terms of cortical thickness with mean pure tone average (mPTA) revealed by ROI analyses with FreeSurfer.

Measure		**Annotation**	**Max**	**NVts**	**Size (mm²)**	**MNI**			***CWP***	***r***
						X	**Y**	**Z**		
LH	thickness	Heschl's gyrus	-3.18	779	367.28	-51	-15	2	0.0056	-0.44

Note. LH: left hemisphere, Max: log10(p) at peak vertex, NVts: number of vertices above threshold, *CWP*: cluster-wise *p* value of Monte Carlo simulation, *r*: correlation coefficient.

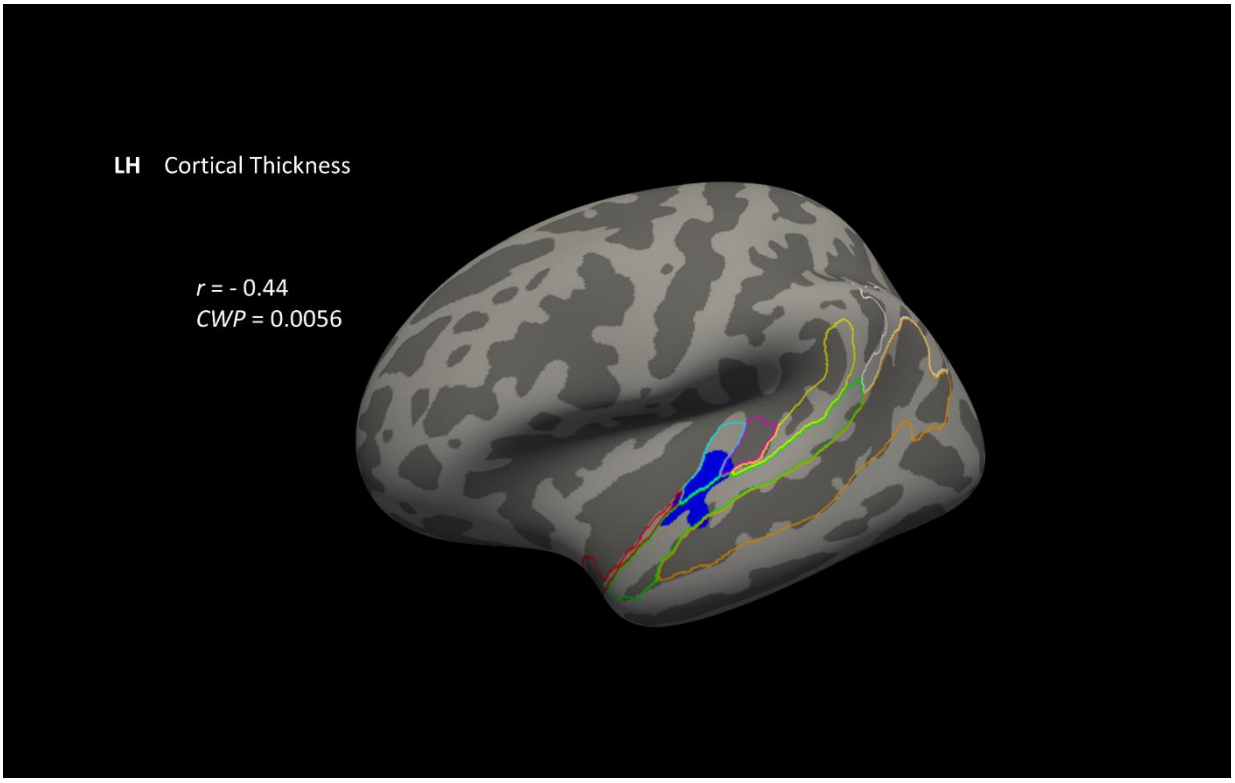

Fig. 5. Cluster in the left transverse temporal region, the cortical thickness of which correlates significantly negatively with mean pure tone average over all participants. ROI annotations according to Destrieuxs aparc.a2009s atlas: light blue = Heschl's gyrus, pink = Heschl's sulcus, red= planum polare, yellow = planum temporale, orange = superior temporal sulcus, green= superior temporal gyrus, white = gyrus angularis. Negative (blue) values are representing a negative correlation between cortical thickness and mPTA. LH = left hemisphere, r= correlation coefficient, CWP = cluster-wise p value.

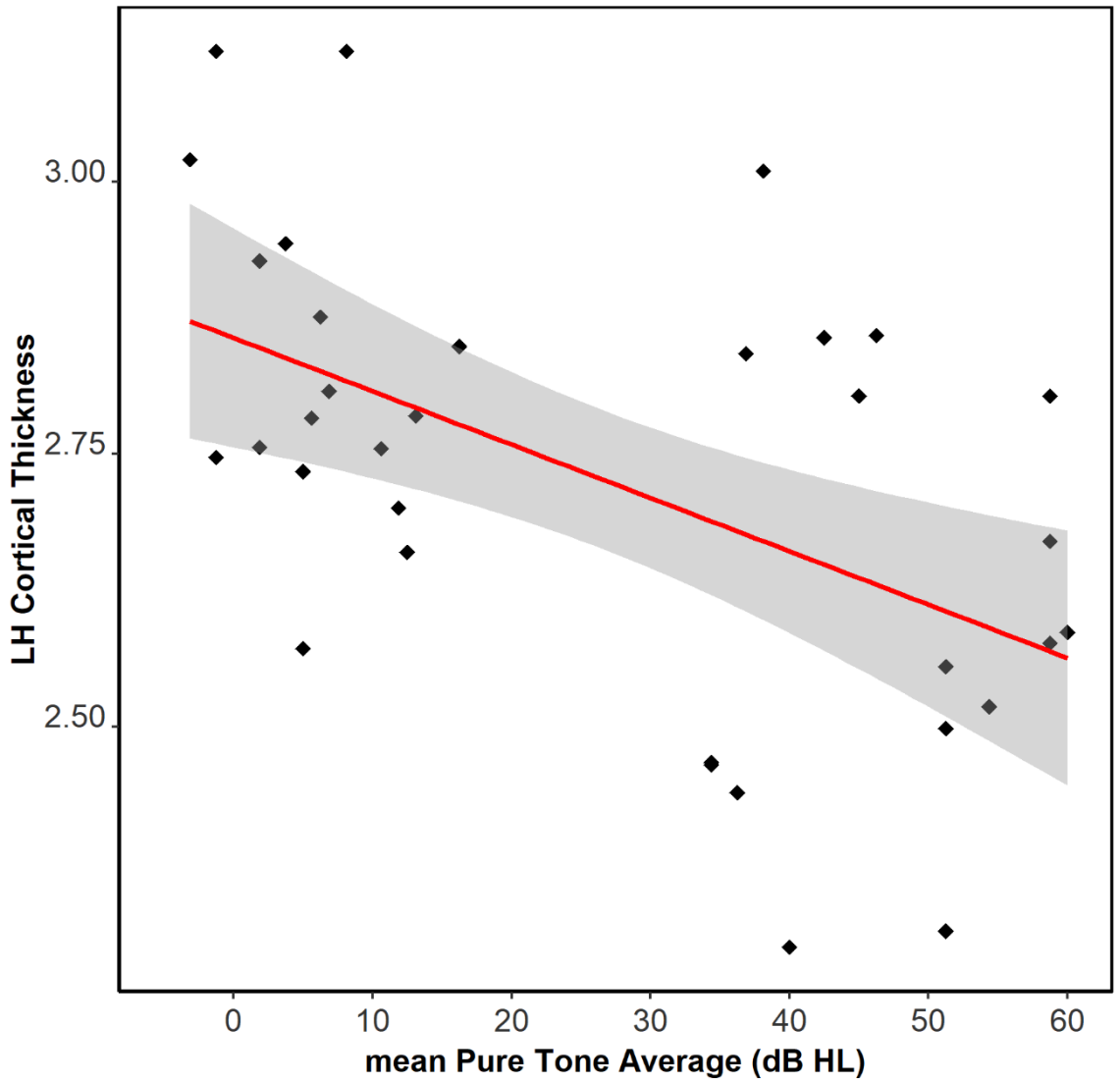

Fig. 6. Relationship between cortical thickness of the left transverse temporal region and hearing acuity (mean pure-tone average at 500, 1000, 2000 and 4000 Hz averaged over both ears) over both groups. In gray, the 95% confidence interval around the linear trend is plotted. LH = left hemisphere.

3.4 Region-Wise Correlation Analysis with Hearing Acuity

The region-wise partial Spearman correlation analysis between the mean CV, CT and CSA of the seven chosen ROIs and the mPTA over all participants with age as control variable revealed a significant negative correlation between CT of the left Heschl's gyrus and the mPTA (r = -0.41, $p_{FDRadj.}$ = 0.034), showing that a thinner Heschl's gyrus correlates negatively with higher hearing thresholds in the left hemisphere. In the same direction, the analysis also revealed a significant negative correlation between CT of the left superior temporal gyrus and the mPTA (r = -0.38, $p_{FDRadj.}$ = 0.03). Taken together, this

region-wise analysis supports the findings of the previous analysis on the vertex level in section 3.3. All significant correlations are shown in Table 5.

Table 5: Significant negative partial Spearman correlation corrected for age, between the mean region-wise CT and mean pure tone average (mPTA in dB) over all participants.

			Thickness *Heschl's gyrus*	**Thickness** *Superior temporal gyrus*
LH	**mPTA**	r	-0.41	-0.38
		$p_{FDRadj.}$	0.034	0.03

Note. LH = left hemisphere, mPTA = mean pure tone average, $p_{FDRadj.}$ = FDR adjusted *p* value, *r*: correlation coefficient.

4. Discussion

In this study, our first goal was to extend the findings of Alfandari et al. (2018) by using another analysis approach, namely surface-based morphometry. In the light of the current stud, the SBM analysis provided new insights into the relationship between hearing acuity and cortical characteristics. Further, we investigated whether the GMV differences reported by Alfandari et al. were driven by differences in CT, CSA, or both. Another aim of this study was to examine to what extent the SBM approach could provide more detailed results as compared to the often-used VBM approach. Lastly, we wanted to replicate the CV findings of Alfandari et al. (2018).

In their VBM study, Alfandari et al. implied a relationship between poorer hearing acuity and increased GM volume in the right angular gyrus. In our study, we were not able to replicate this finding. However, our ROI analysis revealed several other clusters that differed significantly between the two groups, not only in CV, but also in CT and CSA. Even though we also observed differences in the right angular gyrus between the groups, this effect was in the opposite direction when compared to the findings reported by Alfandari et al. (2018). In our analysis, two clusters located in the left and right angular gyrus showed a decreased CV for the HI listeners compared to the NH participants. One possible explanation for the differences in the direction of the effects could be that VBM and SBM operate on different levels (voxel-based vs. vertex-based). Further, VBM has been criticized as being sensitive to image registration procedures and geometrical differences that can result in spurious findings (Bookstein, 2001). In contrast, applying SBM allows the problems associated with registration as well

as geometrical differences to be avoided because this approach uses the cortical folding of the brain and analyzes differences in area, thickness, and the curvature of the cortex between subjects (Winkler et al., 2010). Another important difference between these two approaches is the choice of atlas for the annotation of the ROIs. Alfandari et al. used the automated anatomical labelling (AAL) atlas (Tzourio-Mazoyer et al., 2002) whereas we used Destrieux's a.2009.s annotation (2010). One of these reasons could account for the observed differences in the results between the two studies. Also in contrast to Alfandari et al., our results suggest that the observed decreased measurement values of cortical parameters in the angular gyrus reflects structural degeneration processes rather than compensation mechanisms that may occur in HI individuals. Our other results support this suggested structural degeneration hypothesis such that, in all the auditory clusters found to be significant, the HI group showed lower morphometric values compared to the NH group, regardless of the extracted value (CV, CT or CSA). These findings are in line with previous cross-sectional studies that have already shown that acquired hearing loss is associated with smaller GM and WM volumes, especially in primary auditory cortex areas and the temporal lobe (e.g., Eckert et al., 2012; Husain et al., 2010; Peelle et al., 2011). Further to this, Lin et al. (2014) showed in their longitudinal study that HI participants demonstrated accelerated volume decline in the whole brain as well as in the right temporal lobe (superior, middle, and inferior temporal gyri, and parahippocampus) as compared to the NH participants. In our study, the differences in regional brain structure morphology between the HI and NH group primarily occurred in temporal lobe structures (STG, STS, MTG) that accommodate the core language networks (Friederici, 2011; Friederici, 2012) and in the left angular gyrus that has been implicated in the adaptation to degraded speech (Guediche, Blumstein, Fiez, & Holt, 2014). In addition, our findings partly fall in line with those from the SBM study by Li et al. (2012) that showed significantly less CT in HI compared to NH children and adolescents in the left precentral gyrus, right postcentral gyrus, left superior occipital gyrus and the left fusiform gyrus (Li et al., 2012). Furthermore, the study of Giroud et al. (2018) also revealed that older adults suffering from hidden hearing loss showed reduced CT in auditory-related areas as well as in frontal areas compared to a normal-hearing younger control group. Taken together, our findings indicate that auditory-related cortex areas undergo structural degeneration processes due to distorted auditory input induced by peripheral hearing loss,

independent of age group. However, our analyses did not reveal a relationship between the significant clusters. As already shown by Alfandari et al. (2018), these differed according to participant group as well as level of hearing acuity. Therefore, the data do not demonstrate clear evidence that the morphometric group differences found with our initial vertex-wise group analysis are mainly driven by the different hearing levels between the groups. Thus, the data cannot be construed as directly supporting the association between altered brain structure and partial hearing loss. On the contrary, given the careful matching of the individuals in each of the two groups and the statistical control for age in all analyses, it does not stand to reason to assume that differences in age, education level and/or sex per se account for the differential cortical morphology in auditory-related regions in our sample of normal-hearing and hearing-impaired individuals.

Due to the fact that an SBM analysis with FreeSurfer allowed us to extract not only CV, but also CT and CSA, it is not surprising that our analysis revealed a much more detailed picture of morphometric differences between the two groups compared to the results of the previous VBM study (Alfandari et al., 2018). In addition to the mentioned angular gyrus clusters, we also found differences in middle and superior temporal regions, spread over both the left and right hemispheres. Further, the morphometric differentiation gained through using SBM enabled us to asses whether the observed differences between the groups in terms of CV are driven by differences in CT or CSA. Previous studies that compared the results of VBM and SBM analyses of the same dataset came to the same conclusions as in the current study. For example, Meyer et al. (2016) investigated the difference in neuromorphology associated with tinnitus distress and duration using SBM and compared the results with findings provided by a VBM analysis of that same dataset (Schecklmann et al. 2013). In their study, Meyer and colleagues discovered additional results and differential neuroanatomical alterations of CSA and CT for tinnitus distress and tinnitus duration compared to the VBM results. They concluded that, at the very least, SBM should be used to complement VBM because it allows the assessment of three distinct morphometric parameters, not just CV (Meyer et al., 2016). This should minimize the risk of possible relationships between CT or CSA and behavior being overlooked. In their paper, Gerrits et al. (2016) too found non-overlapping results between their VBM and SBM analyses of the same dataset of Parkinson's disease patients. CSA and CT were differentially affected by the disease and showed diverse associations with cognition. In

addition, the authors mention that a comparison of GMV effects obtained with FreeSurfer and VBM show that the methodological and technical differences between the methods can yield non-overlapping results in the same cohort of participants, and that researchers should be more aware of these differences (Gerrits et al., 2016). Taken together, we support these suggestions of Meyer et al. (2016) and Gerrits et al. (2016).

Nevertheless, in our group analysis we were not able to show any significant relationship between the observed clusters that differed significantly between the two groups and hearing acuity. None of our correlation analyses survived correction for multiple comparisons. One main reason for these findings could be the small sample size of 17 participants per group. This may have lowered the statistical sensitivity of the analysis. Another important aspect that may account for the weak study power is the considerable heterogeneity in etiologies of hearing loss in the HI sample. For example, congenital hearing loss (prelingual) probably affects the development of the cortex and its plasticity differently than age-related hearing loss. In the case of congenital hearing loss for instance, increased cross-modal recruitment of auditory cortices by the other sensory systems, like the visual system, is likely and may result in visual functions that take over and invade auditory regions (e.g., Glick & Sharma, 2017; Petitto et al., 2000). Further to this, Emmorey and colleagues (2003) showed that congenital hearing loss results in less myelination and/or fewer fibers projecting to and from auditory cortices, especially in left and right HG. This circumstance may also limit the identification of additional anatomical correlates of peripheral hearing loss. Because we were aware of these limitations prior to the statistical re-analysis, we performed additional correlation analyses on the vertex-wise as well as on the region-wise level with hearing acuity as a continuous variable in the GLM and age as covariate. This allowed us to partly circumvent and compensate the mentioned limitations of the sample. The results of the vertex-wise analyses revealed a significant cluster in the left HG, extending into neighboring regions. The CT within this cluster correlated significantly negatively with hearing acuity, showing that lower levels of hearing acuity were associated with a thinner cortex, mainly within the left HG. In addition to the left HG, the cluster includes parts of the adjoining left HS, PP, STG and a small part of the STS and thus encompasses the left primary, secondary and tertiary auditory cortex areas. It is not surprising that the largest part of the significant cluster found resides in the left HG. This region (at least, the medially-

situated two-thirds of this cortical stripe) is the location of the human primary auditory cortex (Morosan et al., 2001; Penhune et al., 1996; Rademacher et al., 2001; Zoellner et al., 2019) and several studies have already shown that acquired hearing loss is associated with smaller volume in this area (e.g., Eckert et al., 2012; Peelle et al., 2011). Our results extend these findings and suggest that CT is the main anatomical parameter that accounts for the finding of smaller volume in HG in HI participants. Furthermore, the HG is considered to be particularly important for the coding of basic acoustic cues within language learning (Wong et al., 2008) and seems to be important for language processing, especially in terms of rapid acoustic changes (Warrier et al., 2009). Warrier et al. (2009) also suggested that a larger left HG could be associated with more efficient processing of speech-related cues, which could facilitate the learning and perceiving of new speech sounds. Still further studies associated the HG with pitch processing and auditory learning abilities. In clinical populations with various auditory-related symptoms, neuroanatomical differences in this area were also found; for example, for dyslexia (e.g., Altarelli et al., 2014; Hugdahl et al., 2003), and congenital deafness (e.g., Emmorey et al., 2003; Penhune et al., 2003 According to these studies, our observed correlation between a thinner left HG and increased hearing thresholds seems plausible as the reported cortical thinning occurs in a region important for the perception and processing of relevant phonetic speech cues. If the ability to perceive and process speech is reduced by a disturbed perception of sounds due to peripheral hearing loss, it is reasonable to assume that the brain adapts plastically as a function of these constraints and changes (Lin et al. 2014). Nevertheless, the observed correlations between morphometric parameters and hearing acuity were only found for the left hemisphere, but not for the right. However, a balanced hearing loss in both ears, as shown by the participants in this study, would be expected to be associated with a reduction in morphometric parameters in both the left and the right hemisphere, as it was already demonstrated in a study by Schneider et al. (2009). One possible explanation for the observed results may be the different gyrification of the HG complex in the left and right hemispheres. As shown in studies by Penhune et al. (2003), Dorsaint-Pierre et al. (2006) and Schneider et al. (2009), the left HG complex usually includes a larger first HG compared to the right side. Therefore, morphometric differences may be more visible on the left hemisphere due to the lower variance of morphological parameters compared to the right hemisphere. Unlike Schneider and co-authors (2009) we did not

calculate the HG size at the individual level. Hence, we were not able to evaluate the individual variations in location, gyrification and shape of the HG to the same extent. Actually, we cannot say with confidence that the observed unilateral result is only due anatomical asymmetries of the left and right HG. Nevertheless, the observed significant negative correlation mainly between the thickness of the left HG and hearing acuity supports the interpretation that peripheral hearing loss has negatively affected the morphology of the auditory cortex, most probably through auditory deprivation, regardless of the participants age. This interpretation is additionally supported by the results of our region-wise correlation analysis, which revealed a negative correlation between the thickness of the left HG/STG with hearing acuity, independent of the participants age. As previously mentioned, it has already been demonstrated that CT especially is susceptible to dynamic modulations as induced by training, learning and experience (Bermudez et al. 2009; Engvig et al. 2010). Additionally, age-related changes of the cerebral cortex are expected to be mainly reflected in alterations of CT and not CSA (Meyer et al. 2014; Storsve et al., 2014). Therefore, it is not surprising that the correlation between brain structure and hearing acuity was found for CT only and not for CSA, both in our vertex-wise correlation analysis and in our region-wise analysis.

All of these analyses notwithstanding, one pertinent question remains unanswered. Based on the present data we cannot determine whether the perception of degraded auditory input due to peripheral hearing loss leads to alterations in primary auditory brain structures or vice versa; whether people with reduced CT especially in HG and STG are more vulnerable to hearing loss. While it is plausible that distorted sensory input may have led to alterations in CT in primary and secondary auditory brain areas, longitudinal studies with a much larger group of HI adults are required to reach enough statistical power to confirm this interpretation. Future studies should not only focus on peripheral hearing loss but should also conduct additional hearing assessments, like speech in noise tasks or the measurement of so-called central hearing ability. This ability can be assessed with supra-threshold measurements which reflect temporal compression and frequency selectivity, and thus are able to measure important aspects of spoken language (Lecluyse et al., 2013). Previous studies have already shown that older adults with normal peripheral hearing levels have problems processing speech in noise and show higher central hearing thresholds and altered brain structure compared to normal-hearing younger adults (Giroud et al.,

2018). These insights illustrate the importance of extended measurements when referring to hearing loss and the processing of degraded speech, particularly with regards to influences on the brain. Further, it bares critical reflection whether the traditional clinical classification of hearing loss (e.g., according to the WHO, starting at 25 dB) makes sense. It is our opinion that a modification of the boundaries around this classification would be reasonable; hearing loss should be viewed as an individual continuum with interactions with brain anatomy already in the lower range, and spanning younger to older adults, as indicated by our correlation analysis.

5. Conclusion

The aim of this study was to investigate the relationship between hearing acuity and brain morphology in a HI and NH group with an innovative surface-based morphometry approach to gain more insight into the usage and advantages of different morphometric analysis approaches, and to replicate and extend the findings of Alfandari et al. (2018).

Our vertex-wise group comparison conducted with FreeSurfer revealed several clusters in auditory-related areas that differed between the two groups in terms of CT, CSA and CV. Nevertheless, none of the clusters found correlated significantly with hearing acuity, neither in the NH group nor in the HI group. In all significant clusters, the HI group showed decreased morphometric values compared with the NH group, a result which is opposite to that reported by Alfandari et al. (2018). The additionally conducted vertex-wise correlation analysis between hearing acuity and morphometric parameters over all participants, however, showed one significant cluster in the left transverse temporal region (see Figure 5), encompassing the left Heschl's gyrus, parts of left Heschl's sulcus, parts of the left planum polare, parts of the left superior temporal gyrus and a small part of the left superior temporal sulcus. The CT within this cluster correlated significantly negatively with hearing acuity, showing that higher hearing thresholds were associated with a thinner cortex located mainly within the left HG. The conducted region-wise correlation analysis supported this finding. Taken together, our results suggest that hearing impairment is associated with a reduction of CT in primary, secondary and tertiary auditory cortex regions. These regions are especially involved in perceiving and processing speech cues. This finding has implications not only for older but also for younger and middle-aged adults and is

independent of age-related decline in the cognitive domain as well as in terms of brain structure. Further, our results show that the separate consideration of CV, CT and CSA provides additional information when investigating brain structure and hearing acuity across the lifespan.

6. Acknowledgments

This research was supported by the Swiss National Science Foundation (SNF, Grant no. 105319_169964). The sponsor did not play any role in the analysis and interpretation of the data.

We are indebted to Allison Christen for her helpful comments on this manuscript. During the work on her dissertation, Pia Neuschwander was a pre-doctoral fellow of the International Max Planck Research School on the Life Course.

7. Declarations of interest:

none.

8. Appendix

Table A1: The mean (*M*) and standard deviation (*SD*) of mean cortical volume, separately for hearing-impaired and normal-hearing participants. The *t* tests indicate differences between participant groups.

Measure		Region	Hearing Impaired		Normal Hearing		*t*	$p_{FDRadj.}$
			M	*SD*	*M*	*SD*		
LH	Volume	Superior temporal sulcus	9650.94	694.75	9456.71	1325.12	$t(32) = 0.535$	0.766
		Transverse temporal sulcus	536.71	119.23	564.41	144.23	$t(32) = -0.610$	0.766
		Angular gyrus	5790.71	912.07	5693.77	880.86	$t(32) = 0.315$	0.813
		Heschl's gyrus	950.29	201.19	1076.94	165.38	$t(32) = -2.005$	0.546
		Superior temporal gyrus	5962.06	833.93	6127.65	919.22	$t(32) = -0.550$	0.766
		Planum Polare	1904.00	326.78	1769.24	362.31	$t(32) = 1.139$	0.766
		Planum Temporale	1959.18	321.43	1945.94	413.37	$t(32) = 0.104$	0.918
RH	Volume	Superior temporal sulcus	9339.77	794.50	9669.35	1474.57	$t(32) = -0.811$	0.766
		Transverse temporal sulcus	383.47	80.49	400.94	89.97	$t(32) = -0.597$	0.766
		Angular gyrus	7079.77	949.99	7231.35	708.52	$t(32) = -0.527$	0.766
		Heschl's gyrus	795.47	155.70	818.77	175.19	$t(32) = -0.410$	0.799
		Superior temporal gyrus	5136.53	729.42	5402.18	751.60	$t(32) = -1.046$	0.766
		Planum Polare	2015.41	437.22	2103.06	399.44	$t(32) = -0.610$	0.766
		Planum Temporale	1551.41	262.58	1715.82	263.23	$t(32) = -1.823$	0.546

Note. RH = right hemisphere, LH = left hemisphere, $p_{FDRadj.}$ = FDR adjusted *p* value

Table A2: The mean (*M*) and standard deviation (*SD*) of mean cortical surface area, separately for hearing-impaired and normal-hearing participants. The *t* tests indicate differences between participant groups.

Measure		Region	Hearing Impaired		Normal Hearing		*t*	$p_{FDRadj.}$
			M	*SD*	*M*	*SD*		
LH	Area	Superior temporal sulcus	4052.647	343.108	3934.059	451.382	$t(32) = 0.862$	0.921
		Transverse temporal sulcus	266.941	70.133	271.000	61.152	$t(32) = -0.180$	0.947
		Angular gyrus	1630.588	228.532	1569.059	161.704	$t(32) = 0.906$	0.922
		Heschl's gyrus	320.412	81.001	319.059	49.321	$t(32) = 0.059$	0.953
		Superior temporal gyrus	1335.059	166.355	1284.588	144.586	$t(32) = 0.944$	0.922
		Planum Polare	492.941	71.430	435.824	86.945	$t(32) = 2.093$	0.616
		Planum Temporale	664.471	146.429	656.529	154.072	$t(32) = 0.154$	0.947
RH	Area	Superior temporal sulcus	3979.118	285.043	4001.529	347.933	$t(32) = -0.205$	0.947
		Transverse temporal sulcus	181.176	38.084	184.471	39.989	$t(32) = -0.246$	0.947
		Angular gyrus	1942.000	239.221	1919.471	202.346	$t(32) = 0.296$	0.947
		Heschl's gyrus	245.118	47.203	229.941	45.443	$t(32) = 0.955$	0.922
		Superior temporal gyrus	1205.941	126.944	1215.353	144.342	$t(32) = -0.202$	0.947
		Planum Polare	562.176	131.058	571.647	121.046	$t(32) = -0.219$	0.947
		Planum Temporale	520.353	73.151	557.588	104.919	$t(32) = -1.200$	0.922

Note. RH = right hemisphere, LH = left hemisphere, $p_{FDRadj.}$ = FDR adjusted *p* value

Table A3: The mean (*M*) and standard deviation (*SD*) of mean cortical thickness, separately for hearing-impaired and normal-hearing participants. The *t* tests indicate differences between participant groups.

Measure		Region	Hearing Impaired		Normal Hearing		*t*	$p_{FDRadj.}$
			M	*SD*	*M*	*SD*		
LH	Thickness	Superior temporal sulcus	2.50	0.12	2.53	0.15	$t(32) = -0.553$	0.681
		Transverse temporal sulcus	2.38	0.27	2.47	0.17	$t(32) = -1.166$	0.438
		Angular gyrus	2.69	0.13	2.70	0.18	$t(32) = -0.267$	0.852
		Heschl's gyrus	2.46	0.21	2.66	0.17	$t(32) = -3.068$	0.056
		Superior temporal gyrus	3.08	0.15	3.22	0.18	$t(32) = -2.505$	0.126
		Planum Polare	3.35	0.24	3.52	0.33	$t(32) = -1.639$	0.311
		Planum Temporale	2.65	0.18	2.66	0.14	$t(32) = -0.101$	0.920
RH	Thickness	Superior temporal sulcus	2.49	0.11	2.54	0.17	$t(32) = -0.899$	0.525
		Transverse temporal sulcus	2.49	0.24	2.63	0.26	$t(32) = -1.440$	0.373
		Angular gyrus	2.72	0.15	2.78	0.19	$t(32) = -1.096$	0.437
		Heschl's gyrus	2.52	0.21	2.68	0.23	$t(32) = -2.139$	0.140
		Superior temporal gyrus	3.05	0.18	3.19	0.17	$t(32) = -2.155$	0.140
		Planum Polare	3.26	0.28	3.33	0.25	$t(32) = -0.773$	0.566
		Planum Temporale	2.59	0.12	2.68	0.16	$t(32) = -1.096$	0.437

Note. RH = right hemisphere, LH = left hemisphere, $p_{FDRadj.}$ = FDR adjusted *p* value

8. References

Alfandari, D., Vriend, C., Heslenfeld, D.J., Versfeld, N.J., Kramer, S.E., Zekveld, A.A., 2018. Brain volume differences associated with hearing impairment in adults. Trends in Hearing 22. https://doi.org/10.1177/2331216518763689.

Altarelli, I., Leroy, F., Monzalvo, K., Fluss, J., Billard, C., Dehaene-Lambertz, G., Ramus, F., 2014. Planum temporale asymmetry in developmental dyslexia: revisiting an old question. Hum. Brain Mapp. 35 (12), 5717e5735.

Associated Hearing Care, 2019, March 21. Hearing Loss Is More Complex than Just Not Being Able to Hear. Retrieved from. http://www.associated-hearing.com/about.

Bailey, I.L., Lovie, J.E., 1980. The design and use of a new near vision chart. Optom. Vis. Sci. 57 (6). https://doi.org/10.1097/00006324-198006000-00011.

Benjamini, Y., Hochberg, Y., 1995. Controlling the false discovery rate: a practical and powerful approach to multiple testing. J. R. Stat. Soc. Ser. B 57 (1), 289e300.

Bermudez, P., Lerch, J.P., Evans, A.C., Zatorre, R.J., 2009. Neuroanatomical correlates of musicianship as revealed by cortical thickness and voxel-based morphometry. Cerebr. Cortex 19 (7). https://doi.org/10.1093/cercor/bhn196.

Bookstein, F.L., 2001. "Voxel-based morphometry" should not be used with imperfectly registered images. Neuroimage 14, 1454e1462.

Bosmana, A.J., Smoorenburg, G.F., 1995. Intelligibility of Dutch CVC syllables and sentences for listeners with normal-hearing and with three types of hearing impairment. Int. J. Audiol. 34 (5). https://doi.org/10.3109/00206099509071918.

Boyen, K., Langers, D.R.M., de Kleine, E., van Dijk, P., 2013. Gray matter in the brain: differences associated with tinnitus and hearing loss. Hear. Res. 295, 67e78. https://doi.org/10.1016/j.heares.2012.02.010.

Brodmann, K., 1909. Vergleichende Lokalisationslehre der Grosshirnrinde in ihren Prinzipien dargestellt auf Grund des Zellenbaues. Barth 1e346.

Campain, R., Minckler, J., 1976. A note on the gross configurations of the human auditory cortex. Brain Lang. 3 (2), 318e323.

Cardin, V., 2016. Effects of aging and adult-onset hearing loss on cortical auditory regions. Front. Neurosci. 10. https://doi.org/10.3389/fnins.2016.00199.

Celesia, G.G., 1976. Organization of auditory cortical areas in man. Brain 99 (3), 403e414.

Chang, Y., Lee, S.H., Lee, Y.J., Hwang, M.J., Bae, S.J., Kim, M.N., et al., 2004. Auditory neural pathway evaluation on sensorineural hearing loss using diffusion tensor imaging. Neuroreport 15 (11). https://doi.org/10.1097/01.wnr.0000134584.10207.1a.

Dale, A.M., Sereno, M.I., 1993. Improved localization of cortical activity by combining EEG and MEG with MRI cortical surface reconstruction: a linear approach. J. Cogn. Neurosci. 5 (2). https://doi.org/10.1162/jocn.1993.5.2.162.

Dale, A.M., Fischl, B., Sereno, M.I., 1999. Cortical surface-based analysis: I. Segmentation and surface reconstruction. Neuroimage 9 (2). https://doi.org/10.1006/nimg.1998.0395.

Dale, A., Sereno, M., Fischl, B., Marrett, S., Liu, A., Halgren, E., Segonne, F., 2002. FreeSurfer manual. Neuroimage. https://doi.org/10.1016/j.neuroimage.2012.01.021.

Destrieux, C., Fischl, B., Dale, A., Halgren, E., 2010. Automatic parcellation of human cortical gyri and sulci using standard anatomical nomenclature. Neuroimage 53 (1), 1e15. https://doi.org/10.1016/j.neuroimage.2010.06.010.

Dorsaint-Pierre, R., Penhune, V.B., Watkins, K.E., Neelin, P., Lerch, J.P., Bouffard, M., Zatorre, R.J., 2006. Asymmetries of the planum temporale and Heschl's gyrus: relationship to language lateralization. Brain 129 (5), 1164e1176.

Eckert, M.A., Cute, S.L., Vaden, K.I., Kuchinsky, S.E., Dubno, J.R., 2012. Auditory cortex signs of age-related hearing loss. JARO J. Assoc. Res. Otolaryngol. 13 (5), 703e713. https://doi.org/10.1007/s10162-012-0332-5.

Economo, C.V., Horn, L., 1930. Über Windungsrelief, Maße und Rindenarchitektonik der Supratemporalfläche, ihre individuellen und ihre Seitenunterschiede. Zeitschrift für die gesamte Neurologie und Psychiatrie 130 (1), 678e757.

Emmorey, K., Allen, J., Bruss, J., Schenker, N., Damasio, H., 2003. A morphometric analysis of auditory brain regions in congenitally deaf adults. PNAS 100 (17).

Engvig, A., Fjell, A.M., Westlye, L.T., Moberget, T., Sundseth, O., Larsen, V.A., Walhovd, K.B., 2010. Effects of memory training on cortical thickness in the elderly. Neuroimage 52 (4). https://doi.org/10.1016/j.neuroimage.2010.05.041.

Fischl, B., Dale, A.M., 2000. Measuring the thickness of the human cerebral cortex from magnetic resonance images. Proc. Natl. Acad. Sci. 11050e11055.

Fischl, B., Sereno, M.I., Dale, A.M., 1999. SURFER: a software package for cortical surface-based analysis and visualization. Neuroimage 9.

Fischl, B., 2012. FreeSurfer. Neuroimage 62 (2). https://doi.org/10.1016/j.neuroimage.2012.01.021.

Fischl, B., Sereno, M.I., Dale, A.M., 2002. Cortical surface-based analysis. Neuroimage 9 (2). https://doi.org/10.1006/nimg.1998.0396.

Friederici, A.D., 2011. The brain basis of language processing: from structure to function. Physiol. Rev. 91 (4), 1357e1392.

Friederici, A.D., 2012. The cortical language circuit: from auditory perception to sentence comprehension. Trends Cogn. Sci. 16 (5), 262e268.

Galaburda, A., Sanides, F., 1980. Cytoarchitectonic organization of the human auditory cortex. J. Comp. Neurol. 190 (3), 597e610.

Gerrits, N.J., van Loenhoud, A.C., van den Berg, S.F., Berendse, H.W., Foncke, E.M., Klein, M., van den Heuve, A., 2016. Cortical thickness, surface area and subcortical volume differentially contribute to cognitive heterogeneity in Parkinson's disease. PLoS One 11 (2).

Giroud, N., Hirsiger, S., Muri, R., Kegel, A., Dillier, N., Meyer, M., 2018. Neuroanatomical and resting state EEG power correlates of central hearing loss in older adults. Brain Struct. Funct. 223 (1). https://doi.org/10.1007/s00429-017-1477-0.

Glick, H., Sharma, A., 2017. Cross-modal plasticity in developmental and age-related hearing loss: clinical implications. Hear. Res. 343 https://doi.org/10.1016/j.heares.2016.08.012.

Greve, D.N., 2011. An absolute beginner's guide to surface- and voxel-based morphometric analysis. Intl. Soc. Mag. Reson. Med. 19 (2011).

Guediche, S., Blumstein, S., Fiez, S., Holt, L., 2014. Speech perception under adverse conditions: insights from behavioral, computational, and neuroscience research. Front. Syst. Neurosci. 7 (11).

Hagler, D.J., Saygin, A.P., Sereno, M.I., 2006. Smoothing and cluster thresholding for cortical surface-based group analysis of fMRI data. Neuroimage 33 (4). https:// doi.org/10.1016/j.neuroimage.2006.07.036.

Hayasaka, S., Nichols, T.E., 2003. Validating cluster size inference: random field and permutation methods. Neuroimage 20 (4). https://doi.org/10.1016/j.neuroimage.2003.08.003.

Hugdahl, K., Heiervang, E., Ersland, L., Lundervold, A., Steinmetz, H., Smievoll, A.I., 2003. Significant relation between MR measures of planum temporale area and dichotic processing of syllables in dyslexic children. Neuropsychologia 41 (6). https://doi.org/10.1016/S0028-3932(02)00224-5.

Husain, F.T., Medina, R.E., Davis, C.W., Szymko-Bennett, Y., Simonyan, K., Pajor, N.M., Horwitz, B., 2011. Neuroanatomical changes due to hearing loss and chronic tinnitus: a combined VBM and DTI study. Brain Res. 1369. https://doi.org/10.1016/j.brainres.2010.10.095.

Joshi, V.M., Navlekar, S.K., Reddy, K.J., Kishore, G.R., Kumar, E.C.V., 2012. CT and MR imaging of the inner ear and brain in children with congenital sensorineural hearing loss. RadioGraphics 32 (3). https://doi.org/10.1148/rg.323115073.

Lecluyse, W., Tan, C.M., McFerran, D., Meddis, R., 2013. Acquisition of auditory profiles for good and impaired hearing. Int. J. Audiol. 52 (9), 596e605.

Li, J., Li, W., Xian, J., Li, Y., Liu, Z., Liu, S., He, H., 2012. Cortical thickness analysis and optimized voxel-based morphometry in children and adolescents with prelingually profound sensorineural hearing loss. Brain Res. 1430. https://doi.org/10.1016/j.brainres.2011.09.057.

Liem, F., Hurschler, M.A., J€ancke, L., Meyer, M., 2014. On the planum temporale lateralization in suprasegmental speech perception: evidence from a study investigating behavior, structure, and function. Hum. Brain Mapp. 35 (4). https://doi.org/10.1002/hbm.22291.

Lin, F.R., Ferrucci, L., An, Y., Goh, J.O., Doshi, J., Metter, E.J., Resnick, S.M., 2014. Association of hearing impairment with brain volume changes in older adults. Neuroimage 90. https://doi.org/10.1016/j.neuroimage.2013.12.059.

Marie, D., Jobard, G., Crivello, F., Perchey, G., Petit, L., Mellet, E., Tzourio-Mazoyer, N., 2015. Descriptive anatomy of Heschl's gyri in 430 healthy volunteers, including 198 left-handers. Brain Struct. Funct. 220 (2), 729e743. https://doi.org/10.1007/s00429-013-0680-x.

Meyer, M., Liem, F., Hirsiger, S., J€ancke, L., H€anggi, J., 2013. Cortical surface area and cortical thickness demonstrate differential structural asymmetry in auditoryrelated areas of the human cortex. Cerebr. Cortex 24 (10), 2541e2552.

Meyer, M., Neff, P., Liem, F., Kleinjung, T., Weidt, S., Langguth, B., Schecklmann, M., 2016. Differential tinnitus-related neuroplastic alterations of cortical thickness and surface area. Hear. Res. 342. https://doi.org/10.1016/j.heares.2016.08.016.

Mudar, R.A., Husain, F.T., 2016. Neural alterations in acquired age-related hearing loss. Front. Psychol. 7. https://doi.org/10.3389/fpsyg.2016.00828.

Morosan, P., Rademacher, J., Schleicher, A., Amunts, K., Schormann, T., Zilles, K., 2001. Human primary auditory cortex: cytoarchitectonic subdivisions and mapping into a spatial reference system. Neuroimage 13 (4), 684e701.

Panizzon, M.S., Fennema-Notestine, C., Eyler, L.T., Jernigan, T.L., Prom-Wormley, E., Neale, M., Kremen, W.S., 2009. Distinct genetic influences on cortical surface area and cortical thickness. Cerebr. Cortex 19 (11). https://doi.org/10.1093/cercor/ bhp026.

Peelle, J.E., Troiani, V., Grossman, M., Wingfield, A., 2011. Hearing loss in older adults affects neural systems supporting speech comprehension. J. Neurosci. 31 (35). https://doi.org/10.1523/jneurosci.2559-11.2011.

Penhune, V.B., Cismaru, R., Dorsaint-Pierre, R., Petitto, L.A., Zatorre, R.J., 2003. The morphometry of auditory cortex in the congenitally deaf measured using MRI. Neuroimage 20 (2). https://doi.org/10.1016/S1053-8119(03)00373-2.

Penhune, V.B., Zatorre, R.J., MacDonald, J.D., Evans, A.C., 1996. Interhemispheric anatomical differences in human primary auditory cortex: probabilistic mapping and volume measurement from magnetic resonance scans. Cerebr. Cortex 6 (5), 661e672.

Petitto, L.A., Zatorre, R.J., Gauna, K., Nikelski, E.J., Dostie, D., Evans, A.C., 2000. Speech-like cerebral activity in profoundly deaf people processing signed languages: implications for the neural basis of human language. Proc. Natl. Acad. Sci. 97 (25), 13961e13966.

Pfeifer, R.A., 1920. Myelogenetisch-anatomische Untersuchungen über das kortikale Ende der Hörleitung, vol. 32. BG Teubner.

Profant, O., Skoch, A., Balogov a, Z., Tint era, J., Hlinka, J., Syka, J., 2014. Diffusion tensor imaging and MR morphometry of the central auditory pathway and auditory cortex in aging. Neuroscience 260, 87e97. https://doi.org/10.1016/J.NEUROSCIENCE.2013.12.010.

Rademacher, J., Morosan, P., Schormann, T., Schleicher, A., Werner, C., Freund, H.J., Zilles, K., 2001. Probabilistic mapping and volume measurement of human primary auditory cortex. Neuroimage 13 (4). https://doi.org/10.1006/nimg.2000.0714.

Rakic, P., 1988. Specification of cerebral cortical areas. Science 241, 170e176.

Rakic, P., 1995. A small step for the cell, a giant leap for mankind: a hypothesis of neocortical expansion during evolution. Trends Neurosci. 18, 383e388.

Rakic, P., 2007. The radial edifice of cortical architecture: from neuronal silhouettes to genetic engineering. Brain Res. Rev. 55, 204e219.

Rigters, S.C., Bos, D., Metselaar, M., Roshchupkin, G.V., Baatenburg de Jong, R.J., Ikram, M.A., Goedegebure, A., 2017. Hearing impairment is associated with smaller brain volume in aging. Front. Aging Neurosci. 9 (2). https://doi.org/10.3389/fnagi.2017.00002.

Schecklmann, M., Landgrebe, M., Poeppl, T.B., Kreuzer, P., M€anner, P., Marienhagen, J., Langguth, B., 2013. Neural correlates of tinnitus duration and distress: a positron emission tomography study. Hum. Brain Mapp. 34 (1),233e240.

Schneider, P., Andermann, M., Wengenroth, M., Goebel, R., Flor, H., Rupp, A., Diesch, E., 2009. Reduced volume of Heschl's gyrus in tinnitus. Neuroimage 45 (3), 927e939.

Schneider, P., Scherg, M., Dosch, H.G., Specht, H.J., Gutschalk, A., Rupp, A., 2002. Morphology of Heschl's gyrus reflects enhanced activation in the auditory cortex of musicians. Nat. Neurosci. 5 (7), 688.

Ségonne, F., Dale, A.M., Busa, E., Glessner, M., Salat, D., Hahn, H.K., Fischl, B., 2004. A hybrid approach to the skull stripping problem in MRI. Neuroimage 22 (3). https://doi.org/10.1016/j.neuroimage.2004.03.032.

Shapleske, J., Rossell, S.L., Woodruff, P.W.R., David, A.S., 1999. The planum temporale: a systematic, quantitative review of its structural, functional and clinical significance. Brain Res. Rev. 29 (1), 26e49.

Shargorodsky, J., Curhan, S.G., Curhan, G.C., Eavey, R., 2010. Change in prevalence of hearing loss in US adolescents. Jama 304 (7), 772e778.

Sled, J.G., Zijdenbos, A.P., Evans, A.C., 1998. A nonparametric method for automatic correction of intensity nonuniformity in MRI data. IEEE Trans. Med. Imaging 17 (1). https://doi.org/10.1109/42.668698.

Storsve, A.B., Fjell, A.M., Tamnes, C.K., Westlye, L.T., Overbye, K., Aasland, H.W., Walhovd, K.B., 2014. Differential longitudinal changes in cortical thickness, surface area

and volume across the adult life span: regions of accelerating and decelerating change. J. Neurosci. 34 (25), 8488e8498.

Tzourio-Mazoyer, N., Landeau, B., Papathanassiou, D., Crivello, F., Etard, O., Delcroix, N., Joliot, M., 2002. Automated anatomical labeling of activations in SPM using a macroscopic anatomical parcellation of the MNI MRI single-subject brain. Neuroimage 1 (1), 273e289.

Van Strien, J.W., 1992. Classificatie van links- en rechtshandige proefpersonen (Classification of left- and right-handed subjects. Ned. Tijdschr. Psychol. Haar Grensgebieden 47, 88e92.

Vovk, U., Pernus, F., Likar, B., 2007. A review of methods for correction of intensity inhomogeneity in MRI. IEEE Trans. Med. Imaging 26 (3), 405e421.

Warrier, C., Wong, P., Penhune, V.B., Zatorre, R.J., Parrish, T., Abrams, D., Kraus, N., 2009. Relating structure to function: Heschl's gyrus and acoustic processing. J. Neurosci. 29 (1).

Winkler, A.M., Kochunov, P., Blangero, J., Almasy, L., Zilles, K., Fox, P.T., Glahn, D.C., 2010. Cortical thickness or grey matter volume? The importance of selecting the phenotype for imaging genetics studies. Neuroimage 53 (3), 1135e1146.

Wong, P.C.M., Warrier, C.M., Penhune, V.B., Roy, A.K., Sadehh, A., Parrish, T.B., Zatorre, R.J., 2008. Volume of left Heschl's gyrus and linguistic pitch learning. Cerebr. Cortex 18 (4). https://doi.org/10.1093/cercor/bhm115.

Zoellner, S., Benner, J., Zeidler, B., Seither-Preisler, A., Christiner, M., Seitz, A., Schneider, P., 2019. Reduced cortical thickness in Heschl's gyrus as an in vivo marker for human primary auditory cortex. Hum. Brain Mapp. 40 (4), 1139e1154.